NJC

RSC Publishing

PAPER

View Article Online
View Journal | View Issue

Cite this: *New J. Chem.*, 2013, **37**, 534

Surfactant-free preparation of nickel carbonate hydroxide in aqueous solution and its toxic ion-exchange properties

Yong Jia,[ab] Tao Luo,[a] Xin-Yao Yu,[a] Jin-Huai Liu[a] and Xing-Jiu Huang*[a]

Received (in Victoria, Australia) 8th September 2012,
Accepted 26th November 2012

DOI: 10.1039/c2nj40983f

www.rsc.org/njc

In this paper, we have demonstrated a simple surfactant-free solution method for the synthesis of sea urchin-like nickel carbonate hydroxide, which was characterized by field emission scanning electron microscopy, transmission electron microscopy, X-ray diffraction, thermal gravimetric analysis, nitrogen adsorption–desorption isotherms, X-ray photoelectron spectroscopy (XPS) and Fourier transform infrared spectroscopy (FTIR). Two types of carbonate species, a surface unidentate carbonate-like species and a crystal lattice carbonate species, were proposed based on the FTIR and symmetry analysis. The toxic ion-exchange properties towards As(v), Cd(ii), and Cu(ii) ions were investigated. At pH 5.0, the exchange capacities of Cd(ii) and Cu(ii) ions were 120.5 and 109.3 mg g^{-1}, respectively, through the ion-exchange between nickel ions with them, which was confirmed by XPS. For As(v) ion removal, the maximum exchange capacity was 49.6 mg g^{-1} without any pH adjustment, which should be of importance for water treatment. Furthermore, a novel ion-exchange mechanism between the surface unidentate carbonate-like species and As(v) ions was proposed, which was revealed by XPS and FTIR.

Introduction

The occurrence of toxic ions in natural ground water is a world wide problem. The removal of toxic ions from water has attracted great attention because of their toxicity to the human health. For example, arsenic pollution has been reported in the USA, China, Chile, Bangladesh, Mexico, Argentina, Poland, Canada, Hungary, New Zealand, Japan and India.[1] Up to now, several toxic ion-removal techniques from water have been proposed, such as oxidation, precipitation/coprecipitation, coagulation, adsorption, ion-exchange and reverse osmosis.[1] Among the above removal techniques, the adsorption method plays an important role in the purification of water with trace levels of toxic ions owing to its low cost, treatment stability, and easy operation. Recently, the progress being made in the investigation of nanomaterials has brought us a new opportunity for the removal of toxic ions, which is owed to their high surface area and high content of active surface groups. So, nanoadsorbents have attracted great attentions because of their good adsorption properties.[2–4]

Indeed, the adsorption of toxic ions is an ion-exchange process between the active functional groups on the adsorbent surface and the toxic ions in water. Up to now, the widely reported surface active functional group was the surface hydroxyl groups.[5–8] This type of removal process was based on ion-exchange between the surface hydroxyl groups and the toxic anions, and ion-exchange between the hydrogen atoms of the surface hydroxyl groups and the toxic cations. So, the removal efficiency greatly depended on the pH value of the solution. A low pH value resulted in the protonation of surface hydroxyl groups, which was in favor of the adsorption of toxic anions and was not favorable for the removal of cations. The opposite results will be obtained in toxic ions solution with a high pH value. However, it is difficult and impossible to adjust the pH value of natural ground water. So, some researchers have focused on some new types of surface active functional groups, such as surface carboxylic functional groups,[9–11] to improve the adsorption properties.

In our previous work, we reported the shaped-controlled synthesis of $CdCO_3$ microcrystals using a simple solution strategy, and the corresponding nanoporous CdO was obtained.[12] Herein, based on a similar method, sea urchin-like nickel carbonate hydroxide was prepared in pure water without

[a] *Research Center for Biomimetic Functional Materials and Sensing Devices, Institute of Intelligent Machines, Chinese Academy of Sciences, Hefei 230031, PR China. E-mail: xingjiuhuang@iim.ac.cn; Fax: +86 551 5592420; Tel: +86 551 5591142*

[b] *Department of Pharmacy, Anhui University of Traditional Chinese Medicine, Hefei 230031, PR China*

using any surfactant. Two types of carbonates with different symmetries, which are carbonate ions in the $NiCO_3$ crystal lattice (D_{3h} symmetry) and the surface carbonate-like species (C_{2v} symmetry), were proposed for the first time. Ion-exchange properties and the mechanism were investigated by XPS and FTIR in detail. For arsenic species removal, the maximum adsorption capacity was 49.6 mg g^{-1} without any pH adjustment. A novel ion-exchange mechanism based on the surface carbonate-like species was also proposed for As(v) removal, which was revealed by XPS and FTIR results.

Experimental section

Reagents

All chemicals used were of analytical grade and were purchased from Shanghai Chemical Reagents Company and used without further purification. The As(v) stock solution was prepared with deionized water using $Na_3AsO_4{\cdot}12H_2O$. Cd $(NO_3)_2$ and $Cu(NO_3)_2$ were used to prepare the Cd(II) and Cu(II) stock solutions, respectively. The pH value of the As(v) solution was not adjusted. The pH value of the Cd(II) and Cu(II) stock solutions were adjusted to 5 by addition of HNO_3. The toxic ion working solutions were freshly prepared by diluting the stock solution with deionized water. The concentrations of the toxic ion species were given as elemental concentrations in this study.

Preparation of nickel carbonate hydroxide

In a typical synthesis process, $NiCl_2{\cdot}6H_2O$ and urea were dissolved in 100 mL deionized water to form a transparent solution, in which their concentrations were 0.1 and 0.4 mol L^{-1}, respectively. The above solution was transferred into a conical flask with a stopper, and then heated at 100 °C for 12 h and allowed to cool to room temperature naturally. The resulting green precipitates were collected by centrifugation and washed with deionized water repeatedly until a neutral pH was achieved. The precipitates were then dried at 60 °C.

Characterization

The as-prepared products were characterized by field emission scanning electron microscopy (SEM, FEI Sirion 200 FEG, operated at 10 kV), transmission electron microscopy (TEM, JEOL-2010, operated at 200 kV), X-ray diffraction (XRD, X'Pert ProMPD, Cu Kα radiation, wavelength 1.5418 Å), thermal gravimetric analysis (TGA, Pyris 1, heating rate 10 ° min^{-1} in flow air), and X-ray photoelectron spectroscopy (XPS, VG ESCALAB MKII spectrometer, Mg KR X-ray source, 1253.6 eV, 120 W) analyses. Nitrogen adsorption–desorption measurements for the products were performed using a Micromeritics ASAP 2020 M + C instrument with a degassing temperature of 80 °C, and using Barrett–Emmett–Teller (BET) calculations for the surface area and Barret–Joyner–Halender (BJH) calculations for the pore size distribution.

Adsorption experiments

Batch adsorption experiments were conducted to examine the adsorption isotherm of the toxic ions. The adsorption experiments were carried out in 15 mL polypropylene flasks containing 10 mL of arsenate solution and 0.01 g of adsorbent, and then the flasks were shaken at 150 rpm in a shaker at 25 °C for 24 h. In order to evaluate the adsorption properties of the adsorbent in practical water treatment applications, in the adsorption isotherm experiment, arsenate solution with different concentrations was prepared without any pH value adjustment. After the adsorption experiments, the adsorbent was separated from the solution by centrifugation, and the residual toxic ion concentration in solution was determined by using an inductively coupled plasma atomic emission spectrometer (Jarrell-Ash model ICAP 9000). In the kinetics study of As(v) adsorption on nickel carbonate hydroxide samples, the initial As(v) concentrations were 20.80 mg L^{-1}. The adsorbent dose was 1.0 g L^{-1} in the kinetics study. The samples were placed on a shaker for stirring. At predetermined time intervals, stirring was interrupted while 6 mL of the supernatant solution was pipetted and centrifuged for the determination of the remaining As(v) concentration.

Results and discussion

Structures of the nickel carbonate hydroxide

Fig. 1a and b are the SEM images of the as-prepared products. It is clear that sea urchin-like products with 1–2 μm in diameter were obtained. The products were connected together, which was confirmed by the TEM image shown in Fig. 1c. Furthermore, large amounts of thin nanoplates were observed on the surface of the products, as shown in Fig. 1d. The XRD pattern shown in Fig. 2a suggests that the obtained product was nickel carbonate hydroxide $[Ni_2CO_3(OH)_2]$ (JCPDS 35-0501). Recently, Xiao and Yang reported the synthesis of nanoplate-based flower-like $Ni_2CO_3(OH)_2$ spheres in a Teflon-lined stainless autoclave.[13] The size of the obtained nanoplates was greater than 100 nm. In the present work, at the same temperature, sea urchin-like $Ni_2CO_3(OH)_2$ composites of several thin nanoplates were obtained. The results mean that the high pressure in a sealed reaction system was favorable for the growth of the

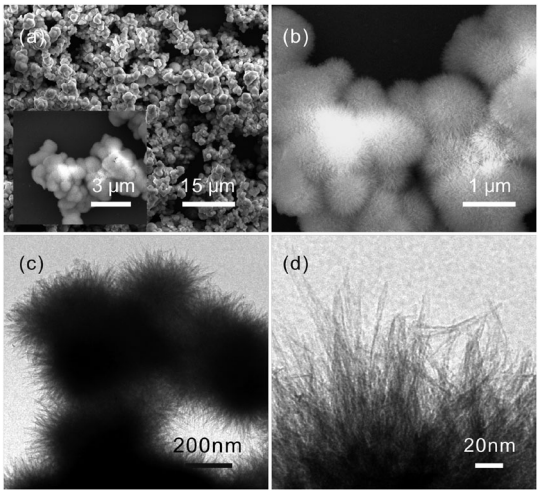

Fig. 1 SEM (a, b) and TEM (c, d) images of the obtained sea urchin-like products.

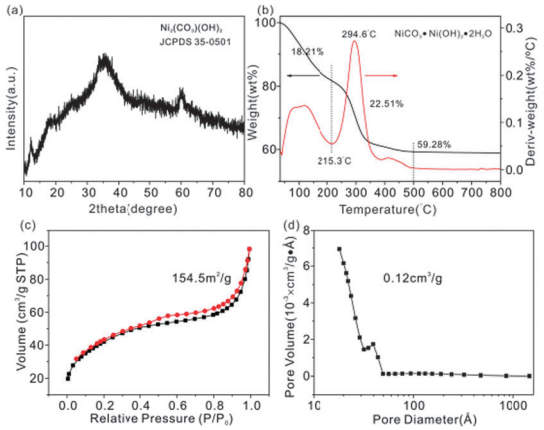

Fig. 2 XRD pattern (a), TGA and DTG curves (b), nitrogen adsorption–desorption isotherm (c), and the pore-size distribution curve (d) of the obtained sea urchin-like nickel carbonate hydroxide.

nanoplates. The wide diffraction peaks shown in Fig. 2a also confirms the small crystal size of the as-prepared products.

The thermal stability of the sea urchin-like $Ni_2CO_3(OH)_2$ was investigated, and the results are shown in Fig. 2b. After calcination in air, the weight content of the obtained NiO was 59.28 wt%. Considering the molecular weights of NiO and $Ni_2CO_3(OH)_2$, the weight content of $Ni_2CO_3(OH)_2$ in the as-prepared product was 83.88 wt%. The residual weight content of 16.12 wt% should be attributed to the crystal water and some physically absorbed water. So, the obtained product was hydrated basic nickel carbonate, and its molecular formula could be $NiCO_3{\cdot}Ni(OH)_2{\cdot}2H_2O$. From Fig. 2b, two weight loss processes are observed. The weight loss between 215.3 and 500 °C should be related to the $Ni_2CO_3(OH)_2$, with a corresponding weight loss of 22.51 wt%. The wide weight loss of 18.21% below 215.3 °C results from the crystal water and some physically absorbed water. The weight loss contents were very close to the calculated results above, and were similar to the previous reports.[14] Nitrogen adsorption–desorption isotherms and the pore-size distribution curve are shown in Fig. 2c and d. The BET surface area and BJH pore volume were 154.5 $m^2\ g^{-1}$ and 0.12 $cm^3\ g^{-1}$, respectively.

Ion-exchange property and mechanism

The removal property of the as-prepared urchin-like nickel carbonate hydroxide towards toxic ions [As(v), Cd(ii), and Cu(ii)] has been investigated. As(v) adsorption experiments were performed without any pH adjustment. We believe that the adsorption capacities are more attractive in practical water treatment applications, and the adsorption isotherm is shown in Fig. 3a. The Langmuir equation was used to model the data, the maximum adsorption capacity of As(v) was 49.6 mg g^{-1}, which was much higher than the values of iron oxide,[3,15] ceria,[16] CuO,[17] and Mn_3O_4,[18] while it was lower than that of Mg/Al layered double hydroxide[19] and MgO.[20] From Fig. 3b, the maximum adsorption capacities of Cd(ii) and Cu(ii) were 120.5 and 109.3 mg g^{-1}, respectively.

The kinetics of adsorption is one of the most important characteristics that define the efficiency of adsorption.

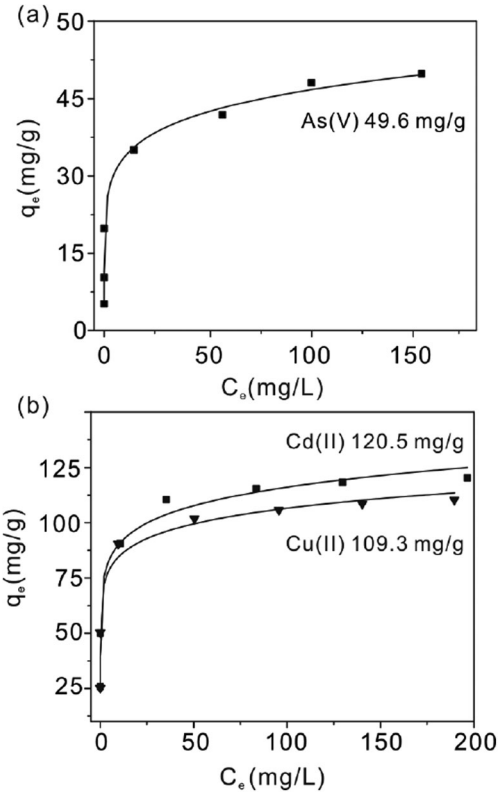

Fig. 3 Adsorption isotherms of As(v), Cd(ii), and Cu(ii).

The kinetics of As(v) adsorption (initial concentration of 20.80 mg L^{-1}) onto urchin-like nickel carbonate hydroxide is shown in Fig. 4a. It is clear that the adsorption rate of As(v) is very fast. Most of As(v) could be removed after 2 h. In addition, the adsorption kinetics experimental data can be fitted into a pseudo-second-order rate kinetic model. The pseudo-second-order model is presented as follows:

$$\frac{t}{q_t} = \frac{1}{k_2 q_e^2} + \frac{1}{q_e} t$$

where k_2 is the rate constant of the pseudo-second-order model of adsorption, q_t is the amount of As(v) adsorbed on the surface of the adsorbent at time t, and q_e is the equilibrium adsorption capacity. For the pseudo-second-order model, the values of k_2 and q_e can be obtained by a plot of t/q_t against t. The pseudo-second-order kinetics plot for the adsorption of As(v) of the adsorbent is shown in Fig. 4b. The results suggest that the experimental data could be well fitted with the linear form of the pseudo-second-order model with a correlation coefficient value of 0.999, which suggests that the pseudo-second-order model represents the adsorption kinetics in the adsorbent systems.

To reveal the As(v) adsorption mechanism, the nickel carbonate hydroxide adsorbent was characterized by FTIR before and after As(v) adsorption, and the results are shown in Fig. 5. The broad absorption band centered at 3440 cm^{-1} was attributed to the O–H bond stretching vibrations, and the band near 1610 cm^{-1} was assigned to the H–O–H bending vibrations.[21] The results imply the

presence of hydroxyl in the products,[22] which was also consistent with the TGA results. The free/uncomplexed state of the carbonate anion in the product belongs to the D_{3h} point group.[23] The FTIR absorption bands at 1076 and 881 cm^{-1} were assigned to the vibrational modes of ν_1 (symmetric stretching) and ν_2 (out-of-plane bending), respectively.[24] The widely reported FTIR absorption band around 1384 cm^{-1} was assigned to the vibrational mode of ν_3 (asymmetric stretching). From Fig. 5, there is a wide FTIR absorption band around 1397 cm^{-1}. So, the band at 1384 cm^{-1} was overlapped. The sharp FTIR absorption band at 832 cm^{-1} was attributed to the vibrational mode of ν_6 (out-of-plane bending).[21,23,25]

However, in Fig. 5, the FTIR absorption bands at 1450 and 1397 cm^{-1} can not be assigned to any of the vibrational modes of the free/uncomplexed state of the carbonate anion in the product. The above two absorption bands were widely attributed to the splitting of ν_3, which results from the decrease of the symmetry from D_{3h} to C_{2v}.[23,25,26] The results suggest that a planar group $CO_2(OX)^-$, which has a C_{2v} symmetry, exists in the as-prepared nickel carbonate hydroxide.[24] Considering the alkaline preparation conditions, the $CO_2(OH)^-$ group was not stable. So, the planar group $CO_2(OX)^-$ in the product should be attributed to $CO_2(ONi)^-$, which is similar to the reported unidentate surface carbonate-like species.[27,28] In addition, the absorption bands at 696 cm^{-1} can be assigned to ρ(OCO) (in-plane rocking vibration).[21,25] Based on the above discussion, we believe that there were two types of carbonate species. The first one was the carbonate ions in the $NiCO_3$ crystal lattice. The second one was the unidentate carbonate-like species on the surface of the products, as shown in Fig. 5.

After As(v) adsorption, the FTIR absorption bands of the carbonate ions in the $NiCO_3$ crystal lattice have no obvious change. However, the FTIR absorption bands at 1450 and 696 cm^{-1} clearly turned weak. At the same time, a new band at 795 cm^{-1} was detected after As(v) adsorption, which can be attributed to the As(v) ions. The results suggest that the carbonate ions in the $NiCO_3$ crystal lattice were not taking part in the ion-exchange process. On the contrary, the surface unidentate carbonate-like species plays a key role in the ion-exchange of the As(v) species. After cation adsorption, it is clear that the FTIR absorption bands of the unidentate carbonate-like species were also weakened. At the same time, a new peak at 1384 cm^{-1} was observed, which may result from adsorbed NO_3^- on the surface. It seems that the unidentate carbonate-like species still participates in the ion-exchange process. However, it should be mentioned that the adsorption of cations was performed at pH 5. So, the reaction between the surface carbonate-like species groups and H^+ in solution should be responsible for the weakened FTIR absorption bands.[29]

In addition, previous reports have been demonstrated that the surface hydroxyl groups of the adsorbent play a key role in As(v) adsorption.[5–8] The exchange between the surface hydroxyl groups and the As(v) species will result in an increased pH value of the solution. To reveal this, in the process of the adsorption kinetics experiment, the influence of the contact time on the pH value was also studied, and the results are shown in Fig. 6. The initial concentration of As(v) solution was 20.80 mg L^{-1},

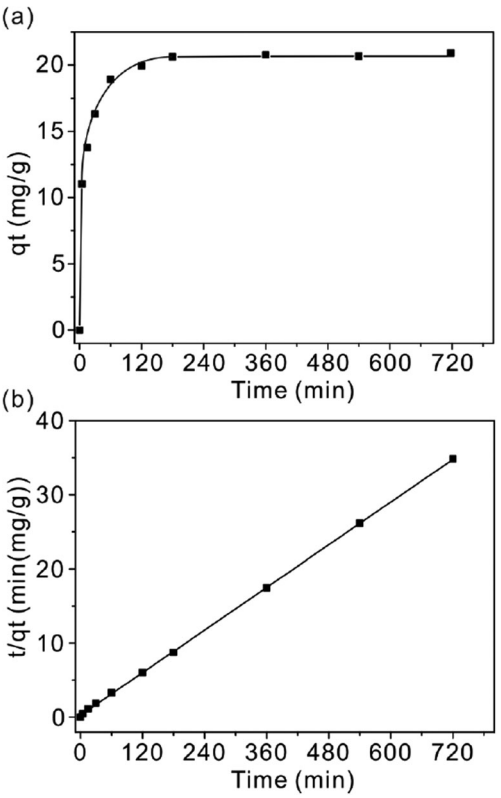

Fig. 4 (a) Effects of contact time on the adsorption of As(v) onto sea urchin-like nickel carbonate hydroxide. (b) Pseudo-second-order kinetic plot for the adsorption of As(v).

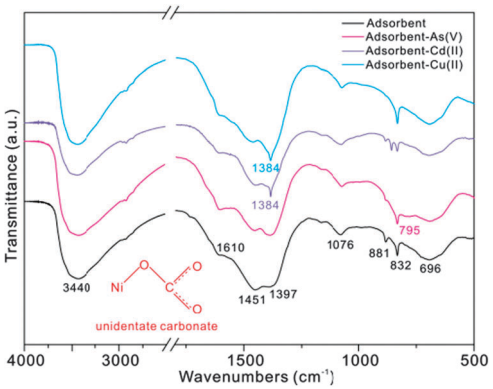

Fig. 5 FTIR spectra of the adsorbent before and after toxic ions adsorption. The inset presents structure the surface unidentate carbonate-like species.

and the pH value of it was 7.73. From Fig. 6, it is clear that the pH value of the solution increased rapidly during the initial two hours, and then gradually achieves a balance. After 12 hours, the pH value of the solution was 8.02. The change of the pH value was consistent with the adsorption kinetics experimental data, which means that the surface hydroxyl groups of the adsorbent also participate in the ion-exchange process.

To further reveal the ion-exchange mechanism, the adsorbent was characterized by XPS before and after the toxic ion-exchange, and the results are shown in Fig. 7. The XPS survey spectra

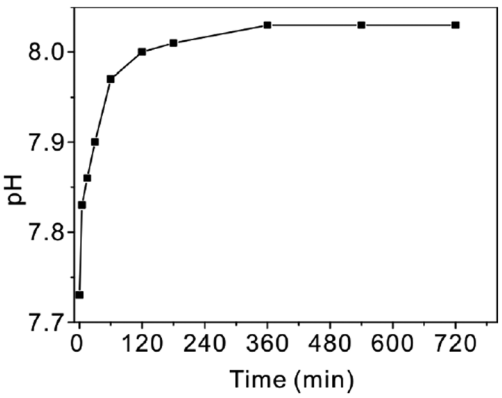

Fig. 6 Effects of contact time on the pH value of the solution.

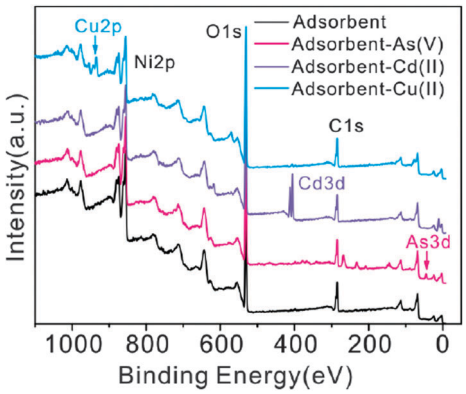

Fig. 7 XPS survey spectra of the adsorbent before and after toxic ion adsorption.

confirmed the existence of the adsorbed toxic ions. The corresponding atom contents before and after adsorption are listed in Table 1. After As(v) adsorption, the atom content of C was obviously decreased. The decreased C content was 2.69 atom%, which was very close to the detected As content of 2.54 atom%. The results further confirmed the key role of the surface carbonate-like species groups. However, after Cd(II) and Cu(II) adsorption, the C atom content did not appear significantly altered. So, the surface carbonate-like species groups were not taking part in the ion-exchange process. On the contrary, the Ni contents were decreased from 19.29 atom% to 17.19 atom% and 15.92 atom%, respectively. The decreased Ni contents were 2.10 atom% and 3.37 atom%, respectively. At the same time, 2.39 atom% of Cd and 3.84 atom% of Cu atoms were detected, which was slightly larger than the decreased Ni atom content. So, the adsorption of toxic cations mainly results from the ion-exchange between nickel ions.

Fig. 8 is the C 1s spectra of the adsorbent before and after As(v) adsorption. For the adsorbent, the peak at 289.3 eV can be assigned to the surface carbonate-like species groups.[28,30] After As(v) adsorption, the content decreased from 24.87% to 18.85%. In combination with the total carbon atom content of the adsorbent shown in Table 1, the content of the surface carbonate-like species groups was 7.22 atom%. After As(v) adsorption, the content of the surface carbonate-like species

Table 1 Atom contents of the adsorbent before and after toxic ion adsorption

	Ni	C	O	As	Cd	Cu
Adsorbent	19.29	29.04	51.67	—	—	—
Adsorbent-As(v)	20.21	26.35 ΔC/2.69	50.90	2.54	—	—
Adsorbent-Cd(II)	17.19 ΔNi/2.10	28.89	51.53	—	2.39	—
Adsorbent-Cu(II)	15.92 ΔNi/3.37	29.06	51.18	—	—	3.84

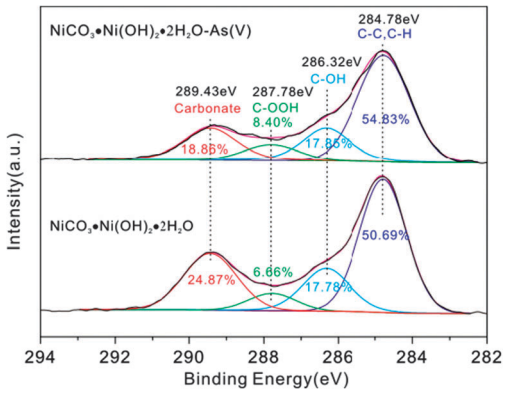

Fig. 8 XPS C 1s spectra (a) of the adsorbent before and after As(v) adsorption.

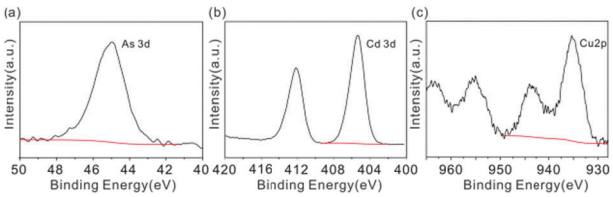

Fig. 9 XPS As 3d (a), Cd 3d (b), and Cu 2p (c) spectrum of the adsorbent after toxic ions adsorption.

groups was 4.97 atom%. So, the decreased carbon atom content was 2.25%, which was close to the decreased carbon content shown in Table 1. The results further demonstrated the ion-exchange process between the surface carbonate-like groups and As(v) species. Fig. 9 shows the As 3d, Cd 3d, and Cu 2p spectra of the adsorbent after adsorption. The results also confirmed the presence of the adsorbed toxic ions.

Conclusions

Sea urchin-like nickel carbonate hydroxide was prepared using a simple surfactant-free solution method. The carbonate of the as-prepared product was divided into the carbonate ions in the $NiCO_3$ crystal lattice (D_{3h} symmetry) and the surface carbonate-like species (C_{2v} symmetry). The toxic ion-exchange mechanism was investigated. For cations, the ion-exchange occurred between the nickel ions and the toxic metals ions in solution. The surface carbonate-like species and the surface hydroxyl

groups play key roles in As(v) adsorption *via* the ion-exchange mechanism. The proposed novel ion-exchange mechanism, based on the surface carbonate-like species, should be of importance for both theoretical investigations and practical water treatment applications.

Acknowledgements

This work was supported by the Natural Science Foundation of Education Committee of Anhui Province (KJ2012A179), the National Key Scientific Program, Nanoscience and Nanotechnology (2011CB933700), the China Postdoctoral Science Foundation (2011M501073), the Natural Science Foundation of Anhui University of Traditional Chinese Medicine (2011zr017B), and the National Natural Science Foundation of China (21103198, 21073197, 11205204 and 61273066).

Notes and references

1 T. Tuutijärvi, J. Lu, M. Sillanpää and G. Chen, *J. Hazard. Mater.*, 2009, **166**, 1415–1420.
2 D. Mohan and C. U. Pittman, *J. Hazard. Mater.*, 2007, **142**, 1–53.
3 L. S. Zhong, J. S. Hu, H. P. Liang, A. M. Cao, W. G. Song and L. J. Wan, *Adv. Mater.*, 2006, **18**, 2426–2431.
4 L. C. Roberts, S. J. Hug, T. Ruettimann, M. Billah, A. W. Khan and M. T. Rahman, *Environ. Sci. Technol.*, 2004, **38**, 307–315.
5 Y. Zhang, M. Yang, X. M. Dou, H. He and D. S. Wang, *Environ. Sci. Technol.*, 2005, **39**, 7246–7253.
6 G. S. Zhang, J. H. Qu, H. J. Liu, R. P. Liu and G. T. Li, *Environ. Sci. Technol.*, 2007, **41**, 4613–4619.
7 N. N. Nassar, *J. Hazard. Mater.*, 2010, **184**, 538–546.
8 Y. X. Zhang, X. Y. Yu, Z. Jin, Y. Jia, W. H. Xu, T. Luo, B. J. Zhu, J. H. Liu and X. J. Huang, *J. Mater. Chem.*, 2011, **21**, 16550–16557.
9 R. Demir-Cakan, N. Baccile, M. Antonietti and M. M. Titirici, *Chem. Mater.*, 2009, **21**, 484–490.
10 L. Wang, J. Li, Q. Jiang and L. Zhao, *Dalton Trans.*, 2012, **41**, 4544–4551.
11 H. Wang, Y. F. Yu, Q. W. Chen and K. Cheng, *Dalton Trans.*, 2011, **40**, 559–563.
12 Y. Jia, X. Y. Yu, T. Luo, J. H. Liu and X. J. Huang, *RSC Adv.*, 2012, **2**, 10251–10254.
13 J. W. Xiao and S. H. Yang, *RSC Adv.*, 2011, **1**, 588–595.
14 X. S. Xin, Z. Lu, B. B. Zhou, X. Q. Huang, R. B. Zhu, X. Q. Sha, Y. H. Zhang and W. H. Su, *J. Alloys Compd.*, 2007, **427**, 251–255.
15 H. Li, W. Li, Y. J. Zhang, T. S. Wang, B. Wang, W. Xu, L. Jiang, W. G. Song, C. Y. Shu and C. R. Wang, *J. Mater. Chem.*, 2011, **21**, 7878–7881.
16 L. S. Zhong, J. S. Hu, A. M. Cao, Q. Liu, W. G. Song and L. J. Wan, *Chem. Mater.*, 2007, **19**, 1648–1655.
17 C. A. Martinson and K. J. Reddy, *J. Colloid Interface Sci.*, 2009, **336**, 406–411.
18 J. G. Parsons, M. L. Lopez, J. R. Peralta-Videa and J. L. Gardea-Torresdey, *Microchem. J.*, 2009, **91**, 100–106.
19 K. H. Goh, T. T. Lim and Z. L. Dong, *Environ. Sci. Technol.*, 2009, **43**, 2537–2543.
20 X. Y. Yu, T. Luo, Y. Jia, Y. X. Zhang, J. H. Liu and X. J. Huang, *J. Phys. Chem. C*, 2011, **115**, 22242–22250.
21 D. G. Klissurski and E. L. Uzunova, *Chem. Mater.*, 1991, **3**, 1060–1063.
22 J. F. Li, R. Yan, B. Xiao, D. T. Liang and D. H. Lee, *Energy Fuels*, 2008, **22**, 16–23.
23 J. B. Harrison and V. E. Berkheiser, *Clays Clay Miner.*, 1982, **30**, 97–102.
24 C. M. Su and D. L. Suarez, *Clays Clay Miner.*, 1997, **45**, 814–825.
25 R. Xu and H. C. Zeng, *J. Phys. Chem. B*, 2003, **107**, 12643–12649.
26 G. B. Cai, G. X. Zhao, X. K. Wang and S. H. Yu, *J. Phys. Chem. C*, 2010, **114**, 12948–12954.
27 C. Li, Y. Sakata, T. Arai, K. Domen, K. Maruya and T. Onishi, *J. Chem. Soc., Faraday Trans. 1*, 1989, **85**, 929–943.
28 M. Cerruti, C. L. Bianchi, F. Bonino, A. Damin, A. Perardi and C. Morterra, *J. Phys. Chem. B*, 2005, **109**, 14496–14505.
29 Y. Jia, X. Y. Yu, T. Luo, M. Y. Zhang, J. H. Liu and X. J. Huang, *Dalton Trans.*, 2013, DOI: 10.1039/c2dt32522e.
30 A. F. Carley, M. W. Roberts and A. K. Santra, *J. Phys. Chem. B*, 1997, **101**, 9978–9983.